Modified Magnetic Ground State in $NiMn_2O_4$ Thin Films

B. B. Nelson-Cheeseman,[1,*] R. V. Chopdekar,[1] J. M. Iwata,[1] M. F. Toney,[2] E. Arenholz,[3] and Y. Suzuki[1]

[1]*Department of Materials Science and Engineering, University of California, Berkeley, CA 94720*
[2]*Stanford Synchrotron Radiation Lightsource, SLAC National Accelerator Laboratory, Menlo Park, CA 94025*
[3]*Advanced Light Source, Lawrence Berkeley National Laboratory, Berkeley, CA 94720*

(Dated: October 4, 2010)

We demonstrate the stabilization of a magnetic ground state in epitaxial $NiMn_2O_4$ (NMO) thin films not observed in their bulk counterpart. Bulk NMO exhibits a magnetic transition from a paramagnetic phase to a collinear ferrimagnetic moment configuration below 110 K and to a canted moment configuration below 70 K. By contrast, as-grown NMO films exhibit a single magnetic transition at 60 K and annealed films exhibit the magnetic behavior found in bulk. Cation inversion and epitaxial strain are ruled out as possible causes for the new magnetic ground state in the as-grown films. However a decrease in the octahedral Mn^{4+}:Mn^{3+} concentration is observed and likely disrupts the double exchange that produces the magnetic state at intermediate temperatures. X-ray magnetic circular dichroism and bulk magnetometry indicate a canted ferrimagnetic state in all samples at low T. Together these results suggest that the collinear ferrimagnetic state observed in bulk NMO at intermediate temperatures is suppressed in the as grown NMO thin films due to a decrease in octahedral Mn^{4+}, while the canted moment ferrimagnetic ordering is preserved below 60 K.

PACS numbers:

I. INTRODUCTION

Oxide spinels exhibit a wide variety of magnetic configurations in their ground states, including collinear, canted and spiral ferrimagnetic and antiferromagnetic moment structures.[1–4] Recently, there has been renewed interest in spinels with non-collinear moment configurations due to the multiferroicity created by spiral spin modulation.[5,6] In spinels, the intricate network of magnetic exchange interactions between the tetrahedral and octahedral cations through the adjoining oxygen anions results in a wide range of magnetic behavior and depends significantly on the cation valences, cation site occupancies, bond angles and bond lengths present within the material. Altering one or more of these by non-equilibrium preparation techniques or epitaxial thin film strain can cause drastic changes to the magnetic properties, providing opportunities to achieve new magnetic ground states in these materials.[7–11]

$NiMn_2O_4$ (NMO) is an intriguing magnetic material which in bulk exhibits two magnetic transitions as a function of temperature (T_1 = 70 K, T_2 = 110 K) with a collinear moment phase (70 K < T < 110 K) and a canted moment phase (T < 70 K).[4] NMO is known for its applications as a thermistor material,[12] and has recently been identified as an effective spin filter material in Fe_3O_4-based magnetic junctions.[13] When spinel structure NMO is prepared in thin film form by pulsed laser deposition, we find that the resulting films exhibit only one magnetic transition (T = 60 K) as a function of temperature. While it is not uncommon for magnetic materials to exhibit a reduced Curie temperature when prepared in thin film form, the intricate moment interactions present in the bulk form suggests that these non-equilibrium NMO films may exhibit a distinctly different magnetic ground state than their bulk counterparts. This possibility of a new and distinct magnetic material motivates an investigation of these NMO thin films. Furthermore, a detailed understanding of the chemical and magnetic structure of these NMO thin films is important in understanding the behavior of the previous NMO-based magnetic junctions.

Previous work on the magnetism of NMO demonstrates that the bulk magnetism can be profoundly altered by changing the distribution and oxidation state of the Ni and Mn cations, while still maintaining a T_C of 110 K.[4,14–17,19] In general, studies have found that bulk NMO contains Ni^{2+}, Mn^{2+}, Mn^{3+} and Mn^{4+} cations, and cation inversion parameters (ν) ranging from $0.74 < \nu < 0.95$.[4,15,16] For reference, cation inversion is defined along a continuum between $\nu = 0$ ($[Ni]_{Td}[2Mn]_{Oh}O_4$) and $\nu = 1$ ($[Mn]_{Td}[Ni,Mn]_{Oh}O_4$) where T_d and O_h denote tetrahedral and octahedral coordination, respectively. In neutron diffraction of bulk NMO, Boucher et al. examined three bulk samples with different cation inversions (ν = 0.74, 0.80, 0.94), and found that the magnetic moment configurations differ dramatically with cation inversion as a function of temperature and applied magnetic field, while still maintaining the same Curie temperature.[4]

In addition, Lisboa-Filho et al. recently investigated the magnetism of bulk sintered NMO samples, and concluded that the low temperature canted moment phase was controlled by the superexchange between the tetrahedral Mn^{2+} and octahedral Mn^{3+} cations, while the high temperature collinear moment phase was controlled by the double exchange between the octahedral Mn^{3+} and Mn^{4+} cations.[19] In summary, previous work on bulk NMO magnetism demonstrates that any investigation of anomalous magnetic properties in NMO must include studies of the cation inversion and valences.

In this paper, we probe the modified magnetic ground state exhibited by as-grown epitaxial NMO films com-

pared to NMO powder (representative of NMO bulk) and annealed NMO films by investigating the cation oxidation states and site occupancies with element-specific X-ray absorption spectroscopy (XAS), X-ray absorption near-edge structure (XANES) and diffraction anomalous near-edge structure (DANES). We find that although the cation inversion of the as-grown films does not deviate from the bulk, the relative Mn cation valence concentrations on the octahedral sites deviate markedly from that of the bulk and annealed films. Through X-ray magnetic circular dichroism, SQUID magnetometry and resistivity measurements, we see evidence that this change in Mn cation valences modifies the relevant magnetic double exchange interactions which dominate the collinear moment phase. This decrease in octahedral Mn^{4+} results in a selective quenching of the high temperature collinear moment phase in the as-grown films, and demonstrates a means to tune the magnetic ground state in this non-collinear spinel material through altering the cation valence.

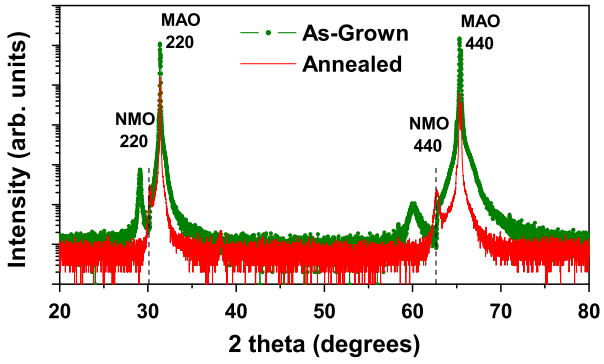

FIG. 1: (Color Online) Specular x-ray diffraction of as-grown and annealed NMO films on (110)-oriented MAO substrates. Dotted lines represent positions of bulk NMO 220 and 440 reflections.

II. EXPERIMENTAL METHODS

$NiMn_2O_4$ thin films were deposited by pulsed laser deposition from a stoichiometric $NiMn_2O_4$ target onto (110)-oriented spinel structure $MgAl_2O_4$ (MAO) and perovskite structure $SrTiO_3$ (STO) and Nb-doped $SrTiO_3$ (Nb:STO) substrates. The NMO thin films were grown at 600 ^{o}C with an energy density of 1.2 J/cm^2 at 10 mTorr of a 99%N_2/1%O_2 gaseous mixture. To highlight any differences in the structure, chemistry, magnetism and resistivity from the as-grown films, the powder from the NMO sintered target and twins of the as-grown NMO films annealed at 800 ^{o}C for 4 hours in air were also studied.

The crystallinity and epitaxy of the as-grown and annealed NMO films on the MAO and STO substrates were characterized by four circle X-ray diffraction with Cu K_α radiation. Synchrotron anomalous diffraction techniques were utilized to obtain the crucial element- and site-specific cation information. Element-specific cation valence information was obtained from L-edge XAS on Beamline (BL) 4.0.2 and BL 6.3.1 at the Advanced Light Source (ALS). L-edge XAS was utilized to determine the relative concentrations of cation valences. Element- and site-specific cation information is obtained from K-edge XANES and DANES on BL 7-2 at the Stanford Synchrotron Radiation Lightsource (SSRL). DANES investigations selectively probe the cation valences populating the crystallographically inequivalent (octahedral and tetrahedral) sites of the spinel crystal structure. Modeling of the DANES spectra provided information on the cation inversion.

The bulk magnetism of the as-grown and annealed NMO thin films and bulk NMO powder was investigated by SQUID magnetometry both as a function of applied magnetic field (up to 5 T) and temperature (5 - 300 K). X-ray magnetic circular dichroism (XMCD) on BL 4.0.2 and BL 6.3.1 at the ALS was utilized to probe the element-specific magnetism as a function of applied magnetic field, temperature and incident x-ray energy to study the specific roles of the various cations on the magnetic behavior of the as-grown and annealed NMO films. The electrical resistance of the highly insulating films was investigated using 2-point probe measurements with a high impedance DC set-up (Keithley 6517A) at 300 K.

III. STRUCTURAL AND CHEMICAL PROPERTIES

A. X-ray Diffraction

The crystal structures of the as-grown and annealed NMO films on both MAO(110) and STO(110) substrates were probed by X-ray diffraction. As seen in Fig. 1, the films exhibit only the spinel (110)-oriented peaks (i.e. (220) and (440)), demonstrating out of plane epitaxy with the MAO (110)-oriented substrates. The same was seen for the as-grown and annealed films on STO and Nb:STO substrates. In-plane alignment of the crystal axes of the NMO films with respect to those of the substrate was confirmed by two-fold symmetry of phi scans of the (400) and (222) peaks of the as-grown and annealed NMO films and the STO(110) and MAO(110) substrates.

For the as-grown NMO films, the out-of-plane lattice parameter was always greater than 8.34 Å (tabulated bulk value of $NiMn_2O_4$) even for 500 nm thick films (8.71 Å).[18] Assuming parameters for NMO similar to Fe_3O_4, the Mathews-Blakeslee critical thickness for lattice mismatch between NMO and STO or MAO gives critical thicknesses much less than 40 Å.[21] Thus, the persistence of an elongated NMO lattice parameter for films

as thick as 500 nm suggests that even with interface dislocations, the film parameter does not converge towards the bulk value and there must be another cause for the structural difference. An increase of lattice parameter with decreasing oxygen content is common in oxide thin films, and has been documented previously in manganite spinels.[20] This trend suggests that the low oxygen growth conditions may cause this elongation in the out-of-plane NMO lattice parameter for all film thicknesses. We note that such lattice distortions could alter the cation-oxygen bond angles and subsequently the relevant magnetic exchange interactions within the as-grown films.[25] Upon annealing in air, the annealed films maintain the epitaxial (110)-orientation of the substrate and recover the bulk $NiMn_2O_4$ out-of-place lattice parameter (8.34 Å), as shown in Fig. 1.

B. L-edge X-ray Absorption Spectroscopy

In order to investigate the chemical valences of the Ni and Mn cations present in the various samples, L-edge XAS was performed. Knowledge of the chemical valences is especially important for the Mn, which has been shown to be present in three different valence states in multiple NMO studies (Mn^{2+}, Mn^{3+}, Mn^{4+}).[15–17] Fig. 2 shows the Ni and Mn L-edge XAS spectra for the NMO powder, as-grown film, and annealed film. The Ni L-edge XAS spectra for all samples indicate a Ni^{2+} state which agrees with earlier NMO investigations.[15–17]

The Mn L-edge spectra for the as-grown films is markedly different from that of bulk and annealed films. The NMO as-grown film spectra in Fig. 2 closely resembles that of well-characterized hausmannite (Mn_3O_4), where the Mn cations are in the following valences and site symmetries: $[Mn^{2+}]_{Td}[2Mn^{3+}]_{Oh}O_4$.[22] This suggests that the as-grown films do not contain a significant concentration of Mn^{4+} as observed in bulk NMO.

Indeed, from Fig. 2, one can see that there is an increase in the absorption intensity at higher photon energies of the Mn L_3 edge in the bulk powder spectra (643 eV), and that this intensity at higher photon energies is also recovered in the annealed films. De Groot et al. have shown that absorption at higher photon energies corresponds to higher Mn valence for Mn L-edge XAS.[23] Fig. 2 clearly shows that the NMO bulk and annealed films show greater absorption at higher energies associated with Mn^{4+}. Thus, we conclude that the as-grown NMO thin films exhibit a dramatic decrease in the relative Mn^{4+} concentration when compared to the bulk, and that this Mn^{4+} concentration is recovered upon annealing the films in air.

C. K-edge X-ray Absorption Near Edge Structure

X-ray absorption near edge structure (XANES) was used at BL 7-2 at SSRL to further investigate the change

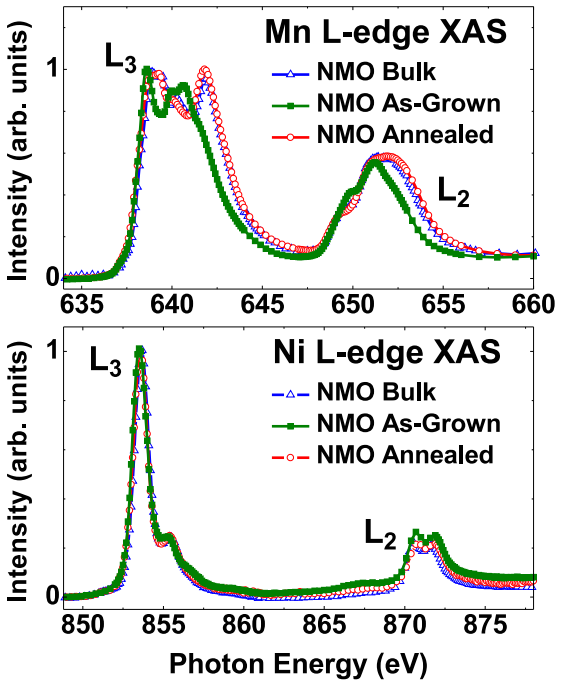

FIG. 2: (Color Online) Ni (top) and Mn (bottom) L-edge XAS of NMO, giving insight into the cation valences present within each sample.

in valence of the Mn cations between the as-grown and annealed NMO films. Fig. 3(a) shows a comparison between the Mn XANES of the as-grown and annealed NMO films. For reference, Fig. 3(b) shows a comparison between two Mn valence- and site-specific standards. $LaMnO_3$ exemplifies the Mn XANES from octahedral Mn^{3+} cations, while $CaMnO_3$ exemplifies the Mn XANES from octahedral Mn^{4+} cations. Fig. 3(c) shows that the absorption edge as well as feature A move to higher energies for higher octahedral Mn valence. Both of these signatures appear in Fig. 3(a) and (b), indicating a transition in the NMO samples from Mn^{3+} to Mn^{4+} upon annealing. Nevertheless, there is still a significant fraction of Mn^{2+} present in the NMO films. These Mn cations also contribute to the Mn XANES spectra and would make any changes to the XANES spectra based on the Mn^{3+} and Mn^{4+} octahedral cations less pronounced.

D. K-edge Anomalous X-ray Scattering

Anomalous X-ray scattering was performed to investigate the cation inversion of the as-grown and annealed NMO films. Here we focus on the 222 reflection of the spinel structure films, as simulations show that this reflection displays a noticeable intensity dependence at the Mn and Ni K-edges depending on the inversion parameter

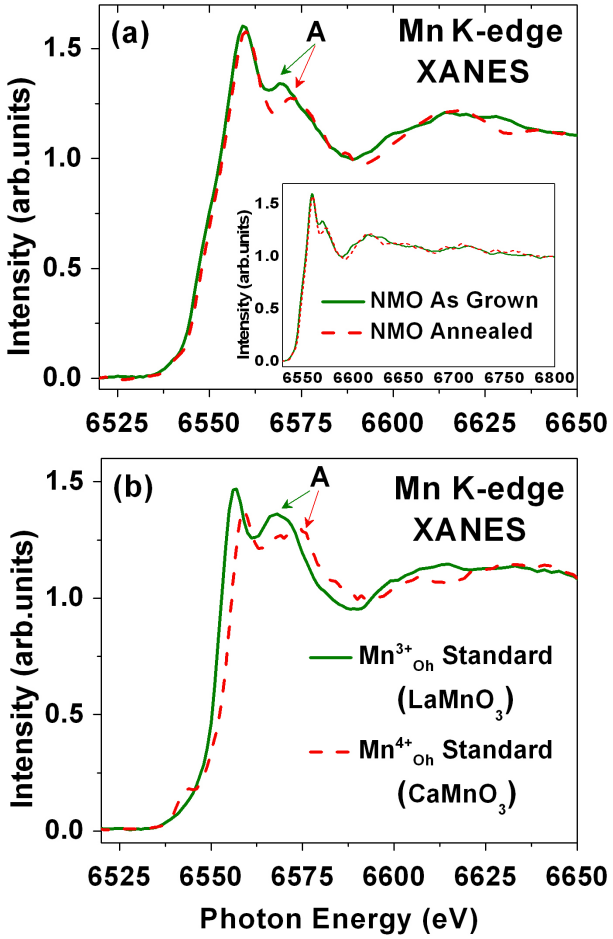

FIG. 3: (Color Online) Mn XANES. (a) Comparison between as-grown and annealed films with feature A marked by arrows. Inset is extended energy range view. (b) Mn valence specific standards illustrating that both absorption edge and feature A shift to higher energy for increasing Mn valence.

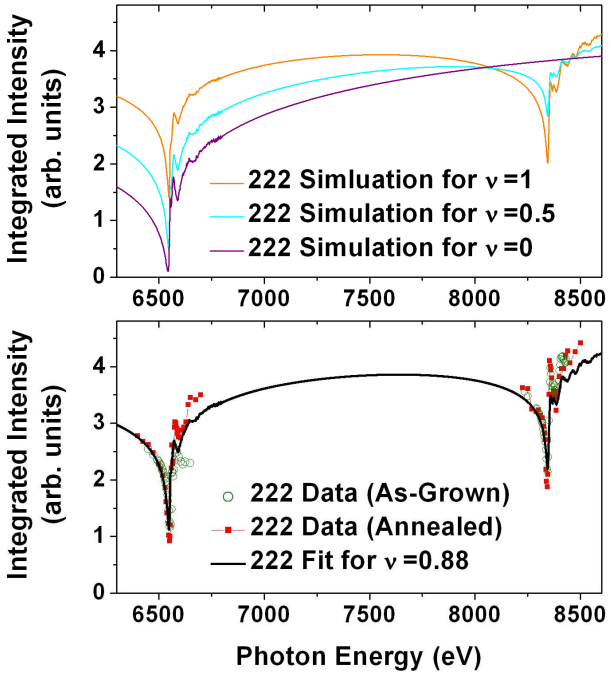

FIG. 4: (Color Online) Anomalous X-ray scattering of NMO 222 reflection. (a) Simulations with inversion parameters ν = 0, 0.5, 1. (b) Data from as-grown and annealed films with nonlinear least square fit of $\nu = 0.88$.

(Fig. 4(a)). The anomalous scattering data for both the as-grown and annealed NMO films is shown in Fig. 4(b). Nonlinear least squared fitting of both data sets with the model gives an inversion parameter of $\nu = 0.88$. Since there are no appreciable changes in the cation inversion between the as-grown and annealed samples, we conclude that the dramatic change in magnetic behavior does not result from differences in cation inversion.

E. K-edge Diffraction Anomalous Near Edge Structure

Diffraction anomalous near edge structure (DANES) was performed to investigate the octahedral site valences of the Mn cations in the as-grown and annealed NMO films. An extensive analysis of the site-specific cation valences of the as-grown NMO films will be presented elsewhere.[24] These studies show that for the as-grown films Mn^{2+} cations dominate the tetrahedral sites, while the octahedral sites are dominated by Mn^{3+}, Mn^{4+} and Ni^{2+} cations.[24] Since the 222 reflection is sensitive to only the octahedral sites within the spinel structure, we examine the Mn 222 DANES to focus on only the Mn valences present on the octahedral sites.[24] Fig. 5 shows key changes in the Mn 222 DANES between the as-grown and annealed NMO films. We see that both the absorption edge energy increases and feature A (also seen in Fig. 3) moves to higher energies for the annealed NMO films. Both of these effects are indicative of a shift to higher Mn valence upon annealing, and correlate with changes seen in Fig. 3 in going from Mn^{3+} to Mn^{4+}. Thus, while the Mn XAS and XANES investigations show a shift to higher overall Mn valence in the annealed films, from the Mn 222 DANES we can directly see that this originates from an increase in the Mn^{4+}:Mn^{3+} concentration on the octahedral sites of the spinel structure. We will see that this directly affects the magnetic interactions in the NMO films. To emphasis these differences, we will subsequently refer to the annealed (as grown) films as the films rich (poor) in octahedral Mn^{4+}.

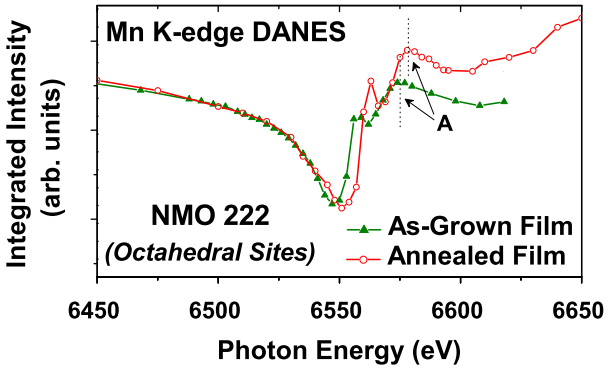

FIG. 5: (Color Online) Mn DANES of the 222 reflection of as-grown and annealed NMO films, indicating a greater concentration of Mn^{4+} cations on the octahedral sites of the annealed film.

IV. MAGNETIC PROPERTIES

A. SQUID Magnetometry

The bulk magnetization of the NMO powder as a function of temperature shows two magnetic transitions at 70 K and 110 K, as shown in Fig. 6. This result is consistent with measurements by Boucher et al. where a star or canted moment was found at low temperatures and evolved into a collinear moment as the temperature was increased through 70 K.[4] In contrast, the bulk magnetization as a function of temperature of the as-grown (Mn^{4+}_{Oh}-poor) NMO thin films shows only one magnetic transition at 60 K and a decreased moment.

The temperature dependence of the magnetization for the bulk, the as-grown (Mn^{4+}_{Oh}-poor) films, and the annealed (Mn^{4+}_{Oh}-rich) films is shown in Fig. 6. At 2 T, the annealed (Mn^{4+}_{Oh}-rich) NMO films exhibit an increased saturation magnetization and increased transition temperature over that of the as-grown (Mn^{4+}_{Oh}-poor) NMO films and closely resemble that of the NMO powder. Additionally, two magnetic transitions as a function of temperature emerge for the 2T data for the annealed (Mn^{4+}_{Oh}-rich) films from the plot of dM/dT (Fig. 6(inset)), again resembling the NMO powder. Thus, the magnetic state of the annealed (Mn^{4+}_{Oh}-rich) NMO films is akin to that of the bulk powder.

The magnetization as a function of temperature for the annealed (Mn^{4+}_{Oh}-rich) films differs remarkably between data taken at 10 Oe and 2 T (Fig. 6(b)). For 10 Oe, the data exhibits a cusped transition at 70 K, suggesting that antiferromagnetic interactions play a key role in the low temperature magnetic phase.[25] Meanwhile, the data taken at 2 T displays magnetic order up to 110 K. Together this suggests the presence of two magnetic phases in the Mn^{4+}_{Oh}-rich films. In order to explore these variations in the magnetic behavior depending on the magnitude of the applied magnetic field, we examine the hysteresis loops of the NMO samples.

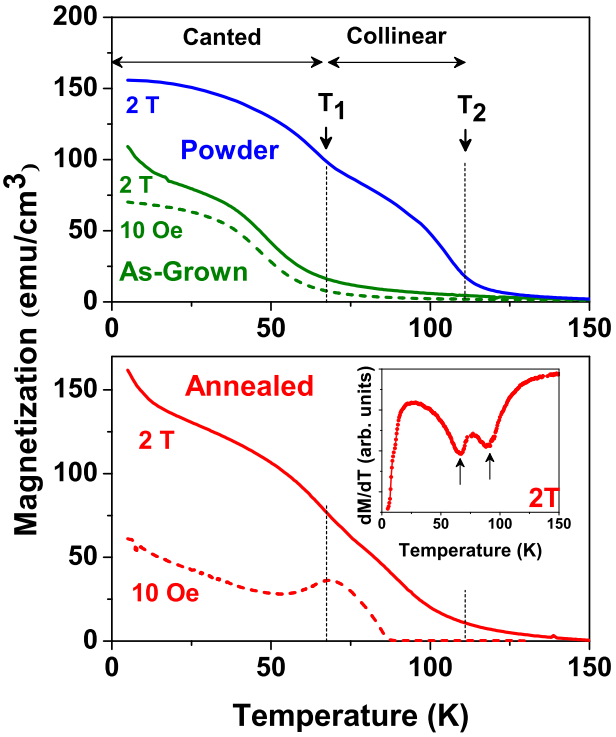

FIG. 6: (Color Online) (top) Magnetization vs. temperature for bulk NMO powder and as-grown (Mn^{4+}_{Oh}-poor) NMO film. (bottom) Magnetization vs. temperature for annealed (Mn^{4+}_{Oh}-rich) NMO film showing two transitions at 2 T and cusped transition at 10 Oe. (inset)Derivative of 2 T curve showing presence of two transitions with temperature. Curves are split into two graphs for clarity.

Hysteresis loops of the as-grown (Mn^{4+}_{Oh}-poor) NMO thin films show a double transition for all temperatures up to the magnetic transition at 60 K (Fig. 7). Such behavior has also been seen in neutron diffraction measurements of bulk NMO and is explained in terms of moment reorientation between the collinear and canted ferrimagnetic states upon application of a magnetic field in the low temperature magnetic phase.[4]

Although the feature of a double transition with field was not observed in the NMO powder samples, it was seen in the annealed NMO film rich in Mn^{4+}_{Oh} (Fig. 8). Interestingly, it is only at low temperatures that hysteresis loops with two coercive fields are seen, while above 70 K the hysteresis loops exhibit only one coercive field. This behavior indicates the presence of the metastable canted and collinear phases at low temperatures and strongly suggests the presence of two magnetic phases as a function of temperature in the annealed (Mn^{4+}_{Oh}-rich) films. The presence of hysteresis loops with two coercive fields for both types of samples at low temperatures indicates a

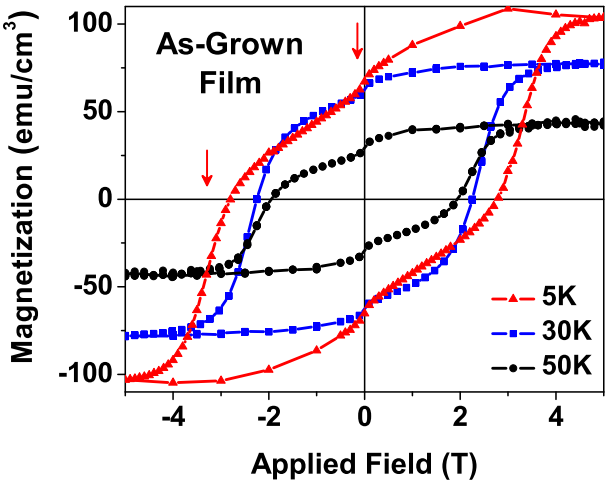

FIG. 7: (Color Online) SQUID hysteresis loops of as-grown (Mn^{4+}_{Oh}-poor) NMO film at various temperatures, showing large coercive fields and double transition hysteresis loops (marked by arrows) for all temperatures.

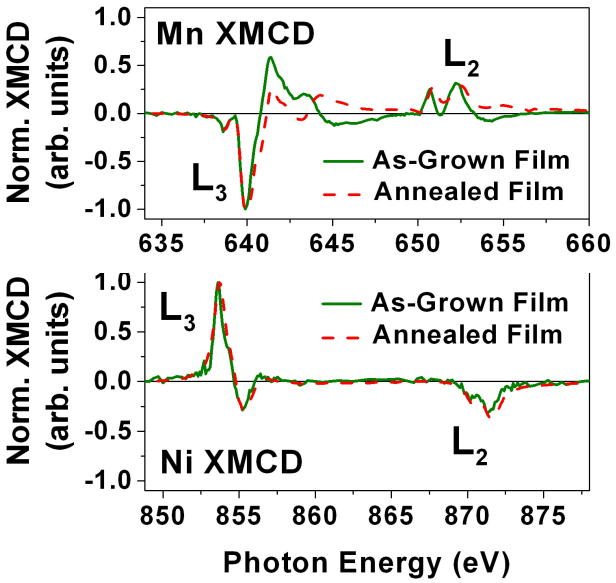

FIG. 9: (Color Online) Mn and Ni XMCD of as-grown (Mn^{4+}_{Oh}-poor) and annealed (Mn^{4+}_{Oh}-rich) NMO films.

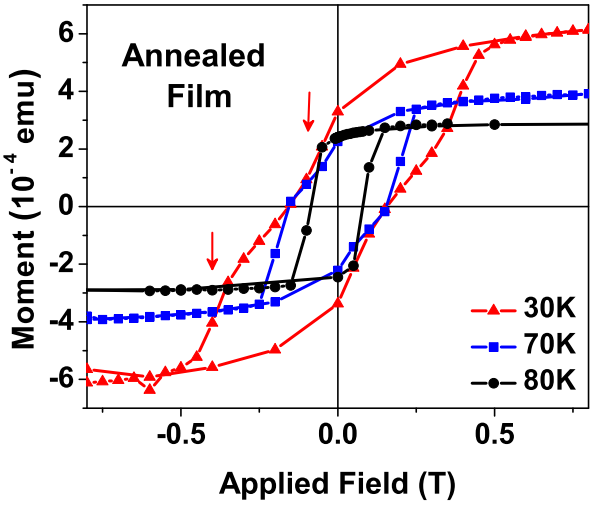

FIG. 8: (Color Online) SQUID hysteresis loops of an annealed (Mn^{4+}_{Oh}-rich) NMO film at various temperatures, showing single and double (arrows) transition hysteresis loops at high and low temperatures, respectively.

similar magnetic state at such temperatures. It also indicates that the collinear phase dominates above 70 K for films rich in Mn^{4+}_{Oh} as seen in bulk,[14] while such a dominant collinear phase is absent in films poor in Mn^{4+}_{Oh}.

Finally, the different temperature-dependent behavior of the annealed (Mn^{4+}_{Oh}-rich) film when taken at two different magnetic fields can be explained in the following way. The low temperature magnetic ground state of the annealed film at H = 0 is a canted phase. One can make the moment collinear at low temperatures by applying a large enough applied field. Thus, at high fields the collinear phase persists to 110 K, while at low fields, the canted phase has a transition at 70 K. In the as-grown (Mn^{4+}_{Oh}-poor) films, the transition temperatures are coincident at 60 K regardless of the magnitude of the applied field indicating a lack of the collinear phase at higher temperatures.

B. X-ray Magnetic Circular Dichroism

In order to better understand the complex magnetism of these NMO films, element-specific X-ray magnetic circular dichroism was carried out. To our knowledge, the complex magnetism exhibited by $NiMn_2O_4$ has not been studied by XMCD before.

The Ni and Mn XMCD spectra of the annealed (Mn^{4+}_{Oh}-rich) sample were probed at 13 K. The Ni XMCD spectrum closely resembles that of $NiFe_2O_4$,[26] where Ni is present as Ni^{2+}_{Oh} (Fig. 9). This result corroborates our chemical investigations (Fig. 2 and 4). Additionally, one can see from Fig. 9 that the Mn dichroism at the lower energies of the Mn L_3 edge (corresponding to the Mn^{2+} cations) is opposite to both the dominant dichroism of the Ni L_3-edge and the dichroism at the higher energies of the Mn L_3 edge (corresponding to the Mn^{3+} and Mn^{4+} cations.) This indicates that the Mn^{2+} cations, shown by DANES to populate the tetrahedral sites, align antiparallel to both the Ni cation moments and the Mn^{3+} and Mn^{4+} cations, all of which predominantly populate the

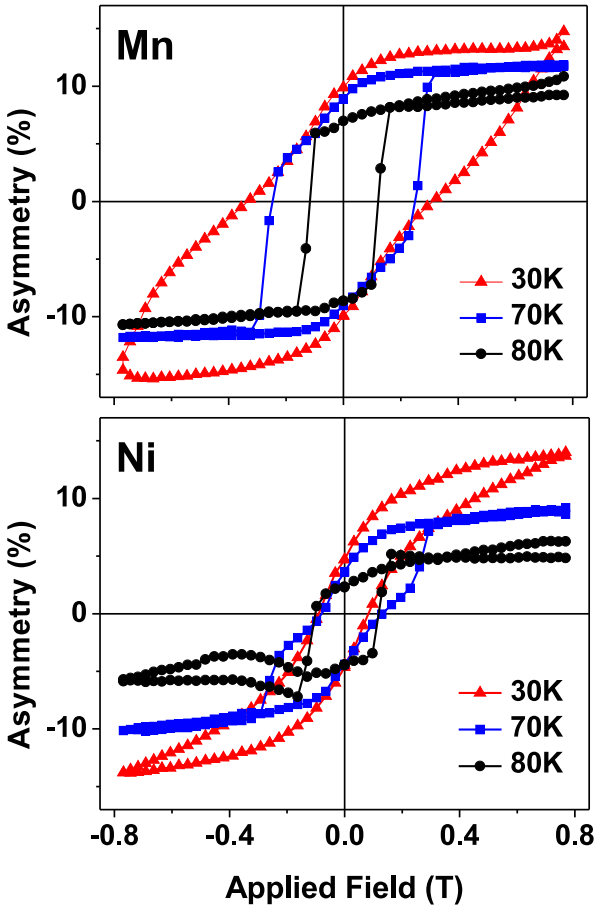

FIG. 10: (Color Online) Mn and Ni XMCD hysteresis loops as a function of temperature for the annealed (Mn^{4+}_{Oh}-rich) NMO film.

octahedral sites.[24] The antiparallel alignment of the octahedral and tetrahedral sublattices is expected in spinel ferrimagnets.

The Ni and Mn XMCD hysteresis loops of the annealed (Mn^{4+}_{Oh}-rich) films as a function of temperature are shown in Fig. 10. We see that at 80 K both the Ni and Mn loops have coincident coercive fields and one distinct switching event, which corroborates the hysteresis loops seen at similar temperatures in the bulk SQUID data for this film. However, as the temperature is lowered through 70 K to 30K, the behavior of the Ni and Mn hysteresis loops deviate dramatically from one another. This indicates a complex magnetic exchange network at low temperatures giving rise to multiple magnetic sublattices which respond differently to the applied magnetic field. This is a key signature of the canted moment state seen at low temperatures in bulk NMO, and is consistent with the presence of multiple magnetic phases (canted and collinear) as a function of temperature for the film rich in Mn^{4+}_{Oh}.

We now examine the Ni and Mn XMCD spectra for the as-grown (Mn^{4+}_{Oh}-poor) film and compare them to that of the annealed (Mn^{4+}_{Oh}-rich) films. Since the as-grown NMO films were highly insulating, epitaxial NMO films were grown on conductive (110)Nb:STO to minimize charging effects. The measurements were performed at 48 K to decrease the coercive field and the film resistivity. The Mn and Ni XMCD spectra for the as-grown film is overlaid with that of the annealed film in Fig. 9. While the Ni XMCD spectra of the two films are coincident, there are marked differences of Mn XMCD lineshapes in the two different film types. More specifically, this evidence suggests that the collinear magnetic state observed in the annealed films can be attributed to the double exchange interaction among the Mn^{3+} and Mn^{4+} cations. One will note that the spectra are coincident at energies associated with the Mn^{2+} cation, but deviate at the energies associated with the Mn^{3+} and Mn^{4+} cations.[23] This suggests that the drastic change seen in the octahedral Mn^{3+} and Mn^{4+} cation valence concentrations can be correlated with the change in the magnetism between the as-grown and annealed films. The large coercive field of the as-grown film resulted in Ni and Mn hysteresis loops that did not saturate with the available 0.75 T capabilities of BL 4.0.2. Therefore, the Ni and Mn moment dynamics could not be deduced from the element-specific hysteresis loops.

Thus, a clear relationship is seen between the site-specific Mn valences determined via chemical and structural measurements in Section III and the magnetic phases seen via magnetic measurements in Section IV. The presence (absence) of octahedral Mn^{4+} results in the presence (absence) of the double exchange interactions between Mn sites on the octahedral sublattice, which results in the presence (absence) of the collinear moment phase found at intermediate temperatures. Meanwhile, the canted moment phase is present at low temperatures regardless of the concentration of octahedral Mn^{4+}, thus indicating it arises from the superexchange interactions commonly found in spinel oxides.

V. TRANSPORT PROPERTIES

In addition to its magnetic signatures, double exchange is also intimately linked to conduction properties in manganites. In order to further assess the double exchange present in NMO samples, we briefly remark on the measured resistance of the as-grown (Mn^{4+}_{Oh}-poor) and annealed (Mn^{4+}_{Oh}-rich) NMO films. Bulk NMO is weakly semiconducting, and although Ni cations also occupy a portion of the octahedral sublattice, the literature finds that the charge transport arises from small polaron hopping between the octahedral Mn^{3+} and Mn^{4+} due to double exchange.[12,27] We find that at room temperature the Mn^{4+}_{Oh}-poor films are highly insulating (9.34 MΩm), while the Mn^{4+}_{Oh}-rich films show several orders of magnitude decrease in resistivity (187 kΩm). A similar decrease in

resistivity with increasing oxygen content is seen in polycrystalline NMO films throughout the literature.[28,29] We outline the following mechanism to explain this. When there is an appreciable presence of octahedral Mn^{4+}, double exchange occurs between the octahedral Mn^{3+} and Mn^{4+} cations, allowing for charge hopping between Mn cations on the octahedral sublattice and a semiconducting behavior. The absence of Mn^{4+} on the octahedral sublattice disrupts the double exchange interactions and, likewise, the charge hopping through the octahedral Mn sites, resulting in a large resistivity. While the Ni cations may play a role in the electrical conduction, we note that the Ni cation valence and distribution are not found to change significantly after annealing (Fig. 2 and 4), while the resistivity does. Therefore, the large change in resistivity between the two films indicates a disruption of the Mn^{3+}-Mn^{4+} double exchange within the as-grown (Mn^{4+}_{Oh}-poor) films, and a trend towards recovery of double exchange in the annealed (Mn^{4+}_{Oh}-rich) films.

VI. CONCLUSIONS

In summary, we have grown single phase epitaxial $NiMn_2O_4$ thin films on (110)-oriented MAO and STO substrates. We observe magnetic properties in the as-grown NMO films that differ greatly from NMO powder and annealed NMO films as a function of temperature. While the bulk powder and annealed films exhibit two magnetic transitions (70 K and 110 K) and two magnetic phases, the as-grown NMO films only exhibit one magnetic transition (60 K) and one magnetic ground state. We find that the cation inversion of the as-grown film does not exhibit a large deviation from bulk values, and film thickness does not appear to play a significant role in the magnetic properties. However, chemical valence analysis shows a decrease in the relative Mn^{4+} concentration on the octahedral sites of the as-grown NMO films compared to bulk powder and annealed NMO films. Such decreases in Mn^{4+} likely disrupt the double exchange interactions that dictate the high temperature collinear magnetic state. This decrease in the Mn^{4+} concentration likely arises from the low oxygen deposition conditions, and results in a selective quenching of the high temperature collinear moment state while preserving the low temperature canted moment state in the as-grown films. Although the change in Mn valence due to annealing is not unexpected, what is revealing is that this valence modification has a dramatic effect on the competing magnetic exchange interactions within this material and results in a new magnetic ground state. This ability to make dramatic changes in the properties of a magnetically-frustrated system via modest changes in cation valence may be more broadly applied to other materials systems with the expectation that new magnetic ground states may be stabilized.

VII. ACKNOWLEDGEMENTS

This work was supported by the National Science Foundation under grant #0604277. R.V.C. was also partly supported by the Director, Office of Science, Office of Basic Energy Sciences (BES), Division of Materials Sciences and Engineering, of the U.S. Department of Energy (DOE) under Contract No. DE-AC02-05CH11231. The ALS is supported by US DOE-BES. Portions of this research were carried out at SSRL, a national user facility operated by Stanford University on behalf of the U.S. Department of Energy, Office of Basic Energy Sciences. B.B.N.C. would also like to acknowledge the support from NSF-IGERT and the Intel Foundation. We would like to thank K.M. Yu for RBS.

* Electronic address: bbnelsonchee@anl.gov

[1] Y. Yafet and C. Kittel. Phys. Rev. **87**, 290 (1952).
[2] N. S. Satya Murthy, M. G. Natera, S. I. Youssee, R. J. Begum, and C. M. Srivastava. Phys. Rev. **181**, 969 (1969).
[3] G. Lawes, B. Melot, K. Page, C. Ederer, M. A. Hayward, Th. Proffen, and R. Seshadri. Phys. Rev. B. **87**, 290 (1952).
[4] P.B. Boucher, R. Buhl, and M. Perrin. J. Phys. Chem. Solids. **31**, 363 (1970).
[5] Y. Yamasaki, S. Miyasaka, Y. Kaneko, J.-P. He, T. Arima, and Y. Tokura. Phys. Rev. Lett. **96**, 207204 (2006).
[6] Y. J. Choi, J. Okamoto, D. J. Huang, K. S. Chao, H. J. Lin, C. T. Chen, M. van Veenendaal, T. A. Kaplan, and S-W. Cheong. Phys. Rev. Lett. **102**, 067601 (2009).
[7] U. Luders, M. Bibes, J.-F. Bobo, M. Cantoni, R. Bertacco and J. Fontcuberta. Phys. Rev. B. **71**, 134419 (2005).
[8] Aria Yang, Z. Chen, Xu Zuo, Dario Arena, J. Kirkland, C. Vittoria, and V. G. Harris. Appl. Phys. Lett. **86**, 252510 (2005).
[9] C. N. Chinnasamy, Aria Yang, S. D. Yoon, Kailin Hsu, M. D. Shultz, E. E. Carpenter, S. Mukerjee, C. Vittoria, and V. G. Harris. J. Appl. Phys. **101**, 09M509 (2007).
[10] F. Rigato, S. Estrade, J. Arbiol, F. Peiro, U. Luders, X. Marti, F. Sanchez, and J. Fontcuberta. Mater. Sci. Engr. B. **144**, 43 (2007).
[11] J. M. Iwata, R. V. Chopdekar, F. J. Wong, B. B. Nelson-Cheeseman, E. Arenholz, and Y. Suzuki. J. Appl. Phys. **105**, 07A905 (2009).
[12] E. D. Macklen, *Thermistors* (Electrochemical Publications, Glasgow, 1979).
[13] B. B. Nelson-Cheeseman, R. V. Chopdekar, L. M. B. Alldredge, J. S. Bettinger, E. Arenholz and Y. Suzuki. Phys. Rev. B. **76**, 220410(R) (2007).
[14] P.B. Boucher, R. Buhl, and M. Perrin. Acta Cryst. **B25**, 2326 (1969).
[15] S. Asbrink, A. Waikowska, M. Drozd, and E. Talik. J. Phys. Chem Solids. **58**, 725 (1997).
[16] V.A.M. Brabers, F.M. van Setten, and P.S.A. Knapen. J. Sol. St. Chem. **49**, 93 (1983).
[17] T. Hashemi and A. W. Brinkman. J. Mater. Res. **7**, 1278 (1992).

[18] R. Legros, R. Metz, and A. Rousset. J. Mater. Sci. **25**, 4410 (1990).
[19] P.N. Lisboa-Filhoa, M. Bahouta, P. Barahonaa, C. Mourec, and O. Pena. J. Phys. Chem. Sol. **66**, 1206 (2005).
[20] Y. Xia, H. Wang, Q. Zhang et al. J. Power Sources. 166, 485 (2007).
[21] L.M.B. Alldredge, R.V. Chopdekar, B.B. Nelson-Cheeseman, and Y. Suzuki. Appl. Phys. Lett. **89**, 182504 (2006).
[22] L.A.J. Garvie, A.J. Craven, and R. Brydson. Amer. Miner. **79**, 411 (1994).
[23] F.M.F. deGroot, J.C. Fuggle, B.T. Thole, and G.A. Sawatzky. Phys. Rev. B. **42**, 5459 (1990).
[24] B.B. Nelson-Cheeseman, R.V. Chopdekar, M. Toney, E. Arenholz, and Y. Suzuki. (Unpublished.)
[25] B. D. Cullity. *Introduction to Magnetic Materials.* Addition-Wesley Publishing Company, Inc., Reading, MA, USA. (1972).
[26] G. van der Laan, C. M. B. Henderson, R. A. D. Pattrick et al., Phys.Rev. B. **59**, 4314 (1999).
[27] N. Tsuda, K. Nasu, A. Fujimori and K. Siratori, in *Electronic Conduction in Oxides*, Solid-State Sciences, edited by M. Cardona *et al.* (Springer, Berlin, 2002).
[28] M. Parlak, T. Hashemi, M.J. Hogan, and A.W. Brinkman. Thin Solid Films. **345**, 307 (1999).
[29] A. Basu, A.W. Brinkman, and R. Schmidt. J. Eur. Cer. Soc. **24**, 1247 (2004).